Scanning tunneling microscopy of silver containing salt of bis(ethylenedithio)tetrathiafulvalene

C. Bai, C. Dai, C. Zhu, Z. Chen, G. Huang, X. Wu, and D. Zhu
Institute of Chemistry, Academia Sinica, Beijing 100080, China

John D. Baldeschwieler
California Institute of Technology, Pasadena, California 91125

(Received 10 July 1989; accepted 25 August 1989)

The surface of silver containing salt of bis(ethylenedithio)tetrathiafulvalene (BEDT-TTF) was studied with the computer-controlled scanning tunneling microscope developed in our laboratory. The crystal surface of the charge-transfer complex is well ordered and a regular array of corrugations is clearly visible. The prominent feature of the experimental scanning tunneling microscopy images is in agreement with the bulk crystal structure obtained by x-ray diffraction method.

I. INTRODUCTION

The sulfur-based organic donor molecule bis(ethylenedithio)tetrathiafulvalene (BEDT-TTF) is known to form a large variety of charge-transfer salts with transport properties ranging from semiconducting, to metallic, to superconducting.[1–3] Some investigations of the BEDT-TTF polyhalides indicate that the extraordinary variety of structures is originated from the different molecular arrangements of BEDT-TTF.[4] Synthesizing new BEDT-TTF charge-transfer salts and studying the correlation between the structure and electronic properties are therefore an interesting subject.

Scanning tunneling microscopy (STM) developed in recent years[5,6] has emerged as a powerful tool for the observation of metal and semiconductor surface in real time with atomic resolution. In contrast, few application of STM to organic materials have been reported. Recently, two papers on STM studies of the organic conductors and superconductors have been published. One described the STM study of the surface of a organic conductor tetrathiafulvalene tetracyanoquinodimethane (TTF-TCNQ),[7] the other was measurements on organic superconductor $(BEDT\text{-}TTF)_2X$ ($X = I_3$, IBr_2, AuI_2). We present here the STM studies on a new BEDT-TTF metallithiocyanate with polymeric anions: $(BEDT\text{-}TTF)Ag_x(SCN)_2 (x \sim 1.6)$.

II. EXPERIMENTS

The crystals were grown in 80 ml 1:1 mixture of 0.052 mmol BEDT-TTF in chlorobenzene with 0.0262 mmol AgSCN and 1.041 mmol Bu_4NSCN in acetonitrile by electrocrystallization. The constant current of 2 μA was applied at room temperature under an atmosphere of Ar gas for a period of about 10 days. The elemental composition of the compound was evaluated using the atomic ratio determined by component analysis.

The crystal of $(BEDT\text{-}TTF)Ag_x(SCN)_2 (x \sim 1.6)$ with dimensions of $0.5 \times 0.5 \times 0.05$ mm was mounted flat on the sample holder of STM with conducting paint. Measurements were made with a STM constructed in our laboratory.

The instrument uses a single-tube three-dimensional scanner with the lowest mechanical resonance at 8 kHz corresponding ot a deflection parallel to the surface of a sample and at 40 kHz corresponding to motion parallel to the tube axis, respectively. The adjusting screws with balls at their ends whose motion is reduced by a system of levers are used in our microscope for the approach or separation of the sample to the tip. Vibration isolation was provided by placing the microscope on the top of a stack of metal plates separated by Viton dampers. This stack is mounted onto double-spring stages with magnetic eddy current damping, like the earlier STM modes in Zurich,[8,9] in order to reduce most of the vibrations to frequencies < 2 Hz. For shielding from electrical noise, we hung the microscope in a metal box and placed the first preamplifier near the tunnel unit to reduce noise.

The STM tip was prepared by placing several millimeters of the lower end of a tungsten wire of 0.5 mm diameter into an aqueous 2N NaOH etching solution and applying a 13 V potential to the tungsten wire with respect to a stainless-steel electrode inserted into the solution. In order to prevent unnecessary etching, we use a shut off circuit to terminate the etching by wire separation. Our STM also uses the AST286 computer for control, data acquisition, and display. The high resolution digital-to-analog converter card and analog-to-digital converter card are used for the computer to generate the voltages applied to the STM piezoelectric elements and to measure the resultant tunneling current. A high resolution graphics controller card is used for real-time display of the STM image. The software that performs the control and data acquisition of the STM has been written in C and lined with some ASSEMBLER subroutines for the critical tasks in order to get a fast and compact executable module which works under DOS Version 3.2. Some image analysis and display tools are included for a posterior image processing.

The STM was operated in the current imaging mode where the tip is scanned at a constant height over the surface and variations in tunneling current are observed. This technique is limited to relatively flat surface, but provides rapid image production and high image quality.

III. RESULTS AND DISCUSSION

Figure 1 shows STM image of the $(BEDT\text{-}TTF)Ag_x(SCN)_2$ surface taken in air at ambient tempera-

 0734-2101/90/010484-04$01.00

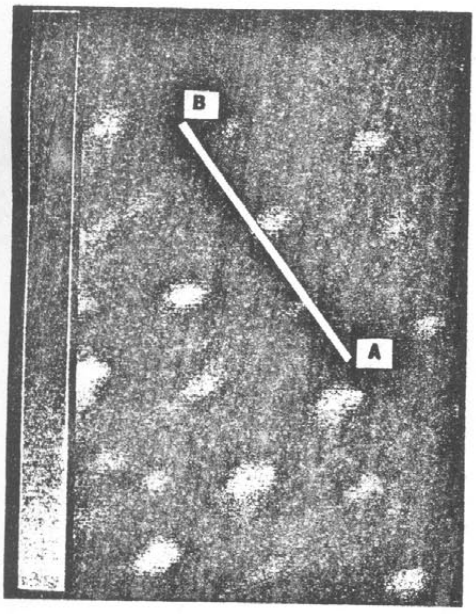

FIG. 1. STM image of the surface of $(BEDT\text{-}TTF)Ag_x(SCN)_2$. The area is 7×17 Å. Lighter regions are higher than darker regions.

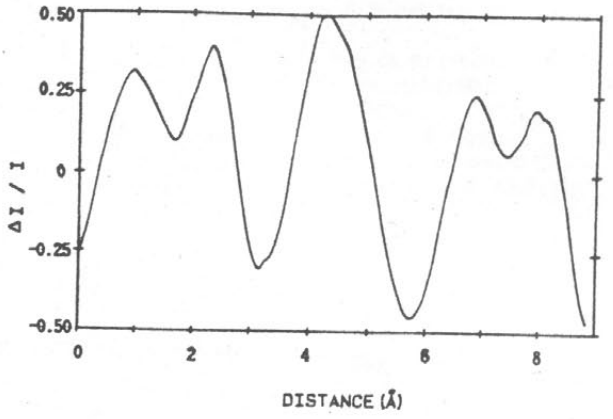

FIG. 2. Interpolated cross section through the data of Fig. 1 along the direction of A–B.

ture and pressure with a tunneling current of 1 nA and a tip bias of + 135 mV relative to the sample. The lateral distance scales in Fig. 1 is those inferred from the nominal expansion coefficients of our piezoelectric ceramic and has not been corrected for piezo nonorthogonality for the time being.

In Fig. 1, a regular array of corrugations is clearly visible. The row of bigger balls and the row of dimers of smaller ball are alternating arrangment on the surface of crystal. The distances between two rows and between two maxima within each row are about 3 and 2 Å, respectively. The variation in tunneling current relative to its mean value along the direction indicated in Fig. 1 is shown in Fig. 2. The interpolated cross section indicates a repeated pattern of dimer balls and single ball. The single peak to hollow corrugation represents a variation of approximately 50% in I/I_0 while the dimer peak to hollow it is less.

The molecular structure of BEDT-TTF is shown in Fig. 3(a). The anion $Ag_x(SCN)$ exists as a polymeric form in this compound, making its STM image difficult to interpret. We have collected the x-ray crystal diffraction data of the title compound on a Nicolet R3m 4-circle diffractometer. The data have been corrected for Lorentz polarization and absorption factors. The crystal is orthorhombic with unit cell parameters $a = 4.253(2)$A, $b = 11.584(4)$A, $c = 40.123(13)$A. The detailed crystal structure has not been solved for the time being. We note that the lattice constants we obtained are in good agreement with those of $(BEDT\text{-}TTF)Ag_x(SCN)_2$ ($x \simeq 1.6$) reported by Geiser *et al.*[10] [$a = 4.257(2)$A, $b = 11.588(3)$A, $c = 40.18(2)$A]. The projections of the crystal structure of $(BEDT\text{-}TTF)Ag_x(SCN)_2$ onto the *bc* plane and *ab* plane are shown in Figs. 3(b) and 3(c), respectively. The crystal structure of $(BEDT\text{-}TTF)Ag_x(SCN)_2$ ($x \sim 1.6$) consists of alternating BEDT-TTF molecule and anion layers, along to the *c* direction. Within each donor layer, there are uniform, widely spaced BEDT-TTF molecular stacks. The polymeric anion consists of a double layer of SCN anions interspersed with Ag cations. The latter are located, almost satistically distributed over four possible sites, in channels formed by the S and N atoms of the thiocyanate entities. Geiser *et al.* have also found other BEDT-TTF salts with complex polymeric anions containing disordered silver sites. According to the crystal shape (the crystal grows favorably along the direction of shorter axes *a* and *b*) and the *a* and *b* lattice constants may be identified with the 4 and 12A repeats in Fig. 1, we presume that the surface observed in our STM images is the *ab* plane.

The prominent feature of Fig. 1 is the appearance of raised rows of bigger balls and rows of dimer of smaller balls. The flanks of each bigger ball link with the row of dimers. In the theory of Tersoff and Hamann,[11] the tunneling current is proportional to the local electron density of states at the Fermi energy and tip position, so that in the fast-scan mode, the vertical scale in an STM image reflects the ac variation in tunneling current relative to its mean value. Comparing the Fig. 1 with the Fig. 3(c), the rows of dimer of smaller balls in Fig. 1 may be assigned to the statistically distributed silver atoms and the rows of bigger balls are centered over S atoms in SCN anions. For the time being, we cannot rule out that which atom's valence orbital is the predominant contribution to the density of states in the experimental image. Thus, one cannot *a priori* ignore the possibility that some molecular orbitals of BEDT-TTF are also responsible for the tunnel current.

It was our experience that, on several occasions, such high-quality images of $(BEDT\text{-}TTF)Ag_x(SCN)_2$ appeared only after scanning a few times over a given area. The scan images on initial approach of the tip to the sample usually shown some characteristic features with some noises. The noisy smoothed out with progressive time may be caused by a "conditioning" of the tip.

IV. CONCLUSIONS

We have used the STM to image the surfaces of a new BEDT-TTF metallothiocyanate with polymeric anion

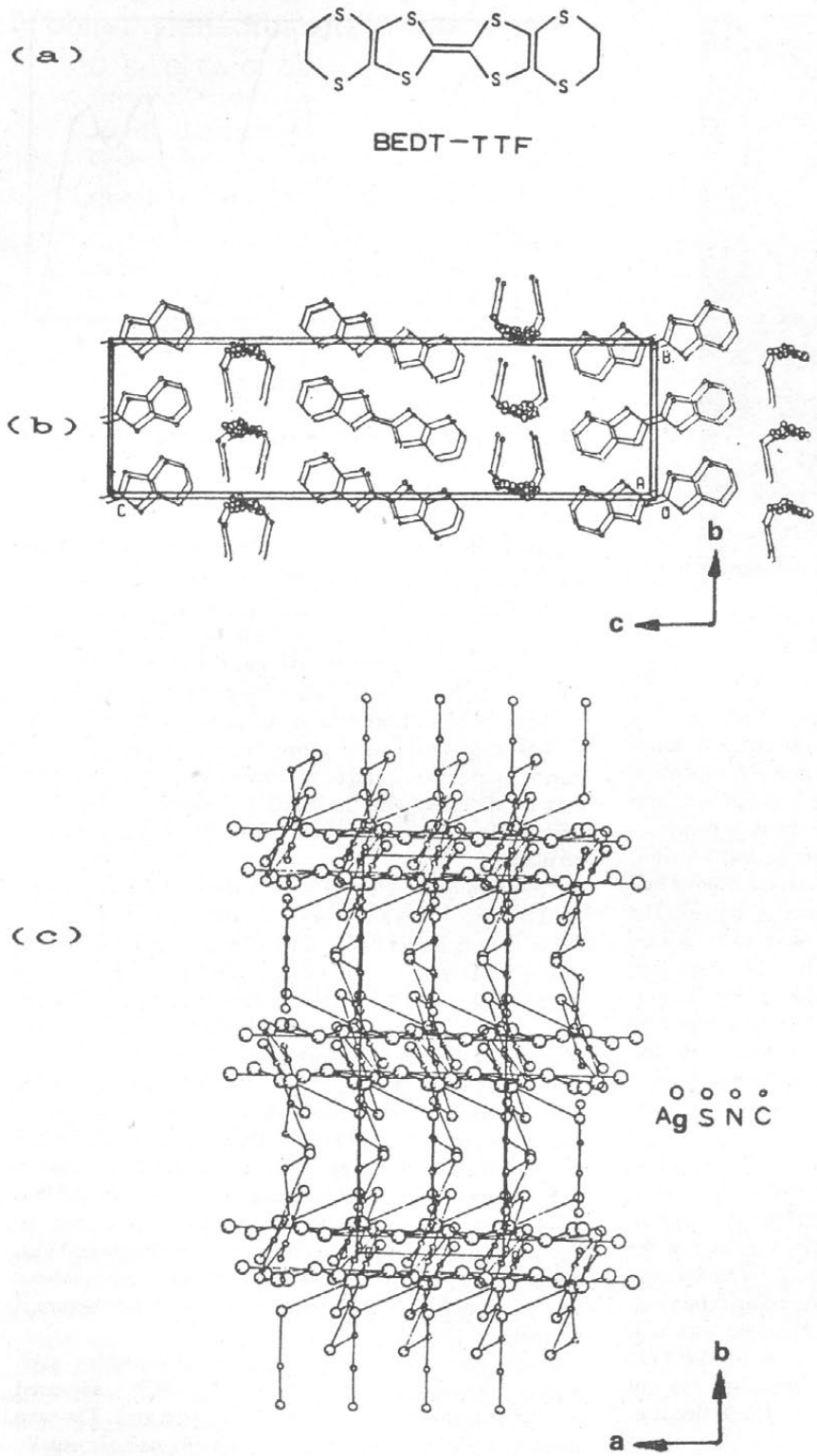

FIG. 3. (a) Molecular structure of BEDT-TTF. (b) Crystal structure viewed slightly off the z axis. (c) The projection of the crystal structure onto ab plane.

$Ag_x(SCN)_2$. The surface of this organic charge-transfer crystal is well ordered. The prominent feature of the experimental STM images agrees with the bulk crystal structure. Further work is required in order to fully understand the electronic behavior of $(BEDT\text{-}TTF)Ag_x(SCN)_2$. This will include some theoretical calculations and I–V measurements and dI/dS maps at room temperature and at low temperature.

[1]J. M. Williams, H. H. Wang, T. J. Emge, U. Geiser, M. A. Beno, P. C. W. Leung, K. D. Carlson, R. J. Thorn, and A. J. Schultz, Prog. Inorg. Chem. **35**, 51 (1987).
[2]P. C. W. Leung, T. J. Emge, A. J. Schultz, M. A. Beno, K. D. Carlson, H. H. Wang, M. A. Firestone, and J. M. Williams, Solid State Commun. **57**, 93 (1986).
[3]H. Kobayashi, R. Kato, A. Kobayashi, Y. Nishio, K. Kajita, and W. Sasaki, Chem. Lett. **789**, 833 (1986).
[4]D. Zhu, P. Wang, M. Wan, Z. Yu, N. Zhu, S. Gärtner, and D. Schweitzer, Physica **143B**, 281 (1986).
[5]G. Binnig, H. Rohrer, Ch. Gerber, and E. Weibel, Appl. Phys. Lett. **40**, 178 (1982).
[6]P. K. Hansma and J. Tersoff, J. Appl. Phys. **61**, R1 (1987).
[7]T. Sleator and R. Tycko, Phys. Rev. Lett. **60**, 1418 (1988).
[8]G. Binnig and H. Rohrer, Sci. Am. **253**, 50 (1983).
[9]G. Binnig and H. Rohrer, Helv. Phys. Acta **55**, 726 (1982).
[10]U. Geiser, M. Beno, A. Kini, H. Wang, A. Schultz, B. Gates, C. Carolyn, S. Cariss, K. Carlson, and J. Williams, Synthetic Metals **27**, A235 (1988).
[11]J. Tersoff and D. R. Hamann, Phys. Rev. B **31**, 805 (1985).